Marine Geology 455 (2023) 106959

Contents lists available at ScienceDirect

Marine Geology

journal homepage: www.elsevier.com/locate/margo

Salt leaching by freshwater and its impact on seafloor stability: An experimental investigation

Nader Saadatkhah [a], Azman Kassim [b], Qurratu Aini Siat [b], Aaron Micallef [a,c,*]

[a] Helmholtz Center for Ocean Research, GEOMAR, Kiel, Germany
[b] Department of Geotechnics and Transportation, School of Civil Engineering, Faculty of Engineering, Universiti Teknologi Malaysia, Johor Bahru 81310 UTM, Johor, Malaysia
[c] Marine Geology and Seafloor Surveying, Department of Geosciences, University of Malta, Msida MSD 2080, Malta

A R T I C L E I N F O

Editor: Michele Rebesco

Keywords:
Offshore freshened groundwater
Salt leaching
Slope instability
Submarine mass movements
Experimental simulations
Numerical modelling

A B S T R A C T

Offshore freshened groundwater (OFG) has been documented in many continental margins worldwide. OFG systems are dynamic, expanding and contracting with falling and rise sea-levels. OFG has long been thought to be an important geomorphic agent in continental margins, either via active discharge at the seafloor, which can erode depressions, or the generation of excess pore pressure, which can deform sediments and cause slope failure. It has also been proposed that OFG flow can drive the loss of sediment shear strength via salt leaching, when seawater in pores is replaced by freshwater. Here, we measure changes in the geotechnical properties of seafloor clayey silt due to salt leaching using flushing experiments, and assess the implications of these changes on the stability of siliciclastic continental margins with 2D limit equilibrium modelling. We document a ~ 50% decrease in undrained cohesive strength of seafloor sediment after flushing, as well as a decrease in its shear strength, bulk density, and moisture content, which is similar to that reported for subaerial quick clays undergoing salt leaching. When applied to a theoretical submarine domain 300 m wide by 100 m high, we estimate that salt leaching can trigger slope failure when the thickness of the flushed layer is >3.5 m or when the slope gradient is >3°. Such conditions are primarily satisfied on the continental slope or the shallow seafloor close to the shoreline. Salt leaching by OFG flow merits consideration as a potential mechanism destablising submarine sedimentary slopes.

1. Introduction

Offshore freshened groundwater (OFG) is water stored in sub-seafloor sediments and rocks with a total dissolved solid concentration below that of seawater. First reported in the 1960s (Kohout, 1964), OFG has now been documented in continental margins worldwide, predominantly in passive siliciclastic margins (Micallef et al., 2021; Post et al., 2013). Meteoric recharge during sea-level lowstands is the most commonly inferred emplacement mechanism (Cohen et al., 2010; Haroon et al., 2021; Kooi et al., 2000; Kooi and Groen, 2001; Micallef et al., 2021; Micallef et al., 2020; Person et al., 2003; Thomas et al., 2019). OFG systems are considered to be dynamic, and their extent expands and contracts with falling and rising global sea-levels. Sea-level has been much lower than today for 80% of the Quaternary period (Bintanja et al., 2005), resulting in the emergence of extensive sections of continental shelf and an increase in hydraulic heads. OFG systems were thus likely more extensive, and associated groundwater fluxes were higher, across continental shelves and slopes, during the majority of the last 2.6 Ma than they are today (Cohen et al., 2010; Faure et al., 2002; Hay and Leslie, 1985; Leahy and Meisler, 1982; Morrissey et al., 2010).

Groundwater flow has long been thought to play a role in a range of seafloor processes shaping continental margins (Johnson, 1939; Stetson and Smith, 1938). This is mainly attributed to: (i) active discharge at the seafloor, which is thought to be responsible for the development of depressions (Goff, 2019; Gwiazda et al., 2018; Hillman et al., 2015; Hoffmann et al., 2020; Hübscher and Borowski, 2006; Idczak et al., 2020; Jakobsson et al., 2020; Jensen et al., 2002; Müller et al., 2011; Puig et al., 2017; Rise et al., 1999; Virtasalo et al., 2019; Whiticar, 2002), or (ii) the generation of excess pore pressure, which can deform sub-seafloor sediments via creep, liquefaction and fluidisation (Bull et al., 2009; Kopf et al., 2016; Moernaut et al., 2017; Nardin et al., 1979)

* Corresponding author at: Department of Geosciences, University of Malta, Msida, MSD 2080, Malta.
E-mail address: aaron.micallef@um.edu.mt (A. Micallef).

https://doi.org/10.1016/j.margeo.2022.106959
Received 30 May 2022; Received in revised form 25 November 2022; Accepted 29 November 2022
Available online 1 December 2022

or may cause slope failure (Kelner et al., 2014; Kopf et al., 2016; L'Heureux et al., 2010; L'Heureux et al., 2012; Oehler et al., 2017; Stegmann et al., 2011; Vanneste et al., 2013). Groundwater flow is also thought to change the physical and chemical properties of sub-seafloor pore fluids. Termed "salt leaching", this process has been proposed to drive the deformation of sub-seafloor sediments offshore Nice (e.g. Dan et al., 2007; Kopf et al., 2016; Stegmann et al., 2011). This concept draws inspiration from studies of subaerial quick clays in Canada and Scandinavia, which are marine clays characterised by very high compressibility and saline pore fluids. Rainwater infiltration and groundwater flow can flush the salts out and reduce the pore water salinity (Bjerrum, 1954; La Rochelle et al., 1970). Such flushing can have profound effects on the geotechnical properties of the clays because it impacts particle alignment and affects electrical interparticle forces. Reported changes in the geotechnical properties of clays include: (a) a reduction in the undrained shear strength, water-holding capacity and Atterberg limits, and (b) an increase in sensitivity (defined as the ratio between peak and residual undrained strength) and compressibility, both of which may ultimately result in liquefaction and slope instability (Barbour and Yang, 1993; Bjerrum, 1954, 1967; Deng et al., 2011; Ismael, 1993; Kim and Do, 2011; Liu et al., 2021; Locat and Demers, 1988; Madadzadeh Toulegilan et al., 2020; Nguyen et al., 2013; Rolfe and Aylmore, 1977; Torrance, 1974; Wu et al., 2021; Zhang et al., 2019). Such changes in geotechnical properties have been reported in subaerial settings, and the effectiveness of salt leaching in driving deformation and instability in seafloor sediments still needs to be evaluated.

In this study we employ laboratory experiments and numerical modelling to determine how salt leaching of sub-seafloor sediments by OFG flow changes their geotechnical properties, and to assess the implications of these changes on the stability of siliciclastic continental margins. Here we focus on clayey silt because it is one of the most common types of seafloor sediment in this kind of margin (Dutkiewicz et al., 2015).

2. Material and methods

2.1. Sample processing and analyses

2.1.1. Samples

Seafloor sediment was collected opportunistically from the Baltic Sea during the oceanographic expedition AL527 on board the *R/V Alkor* in September 2019. The samples were acquired at site AL527–06, at a water depth of 25 m and location 54°02.419′N, 11°04.679′E using a gravity corer. The core section at depths of 52–152 cm below seafloor was used. Samples at this site are not known to be currently affected by OFG flow/seepage, which makes them suitable for our flushing experiments.

2.1.2. Sample analyses

A series of laboratory tests were carried out to characterise the mechanical and hydraulic properties of the gravity core section. These included index tests for moisture content, specific gravity, grain size (sieve analysis, hydrometer), Atterberg limits, and permeability (Table 1). A consolidation test was also run for the undisturbed sediment sample saturated with saline water to quantify the magnitude and rate of volume decrease when a confined sediment specimen is subjected to different vertical pressures. The cohesive strength of the sediment was determined via a triaxial shear test, where undisturbed sediment samples were subjected to different stress levels and drainage conditions. The applied confining pressures ranged from 100 kPa to 600 kPa to simulate the in-situ pressures at a water depth of 10–60 m. The shear strength parameters were determined via an Unconsolidated-Undrained (UU) test during the triaxial tests (Table 1). A Consolidated-Undrained (CU) test was not carried out because it is difficult to consolidate very soft sediment samples. The value obtained for natural moisture content for the sediment sample was higher than the value of its liquid limit (47% and 35.73, respectively), indicating that the soil sample is soft, sensitive and underconsolidating. The sediment sample would not have survived the various stages of the CU test (saturation, consolidation, shearing) in its current state.

Table 1
Tests carried out to characterise the mechanical and hydraulic properties of the gravity core section using ASTM (American Society for Testing and Materials) and AASHTO (The American Association of State Highway and Transportation Officials) standards.

Geotechnical and hydraulic properties	Test	Standard and code
Moisture content	Moisture	ASTM D 2216–98
Total volume, solid volume, and water volume	Density (Unit Weight)	ASTM D7263–09
Particle size distribution	Sieve analysis	ASTM D 422
Particle size distribution (fine grained fraction)	Hydrometer	ASTM D7928
Liquid limit	Atterberg limits tests	ASTM D 4318
Plastic limit	Atterberg limits tests	ASTM D 4318
Plasticity index	Atterberg limits tests	ASTM D 4318
Maximum dry density	Standard Proctor Compaction Test	AASHTO T99 (AASHTO D 698)
Optimum moisture content	Standard Proctor Compaction Test	AASHTO T99 (AASHTO D 698)
Permeability	Constant head method	ASTM D2434
Consolidation and settlement parameters (Cc, Cr)	Oedometer test	ASTM D2435 D2435M - 11
Shear strength	Triaxial shear test	ASTM D4767
Cohesive strength	Triaxial shear test	ASTM D4767

The preparation of the sample for the UU test involved extruding the sediment as a sample 38 mm in diameter and 84 mm in length, and setting it up in the triaxial cell. The sediment specimen was only subjected to the confining pressure inside the triaxial chamber. The pore water pressures were not measured during this test, so the results can only be interpreted in terms of total stress (undrained cohesive strength, c_u). The triaxial tests were carried out on sediment specimens subjected to different confining stresses. While the confining pressure was kept constant, the deviator stress was increased to failure. The UU tests were carried out before and after the flushing experiments.

Energy Dispersive X-ray (EDX) measurements were carried out on five sediment samples before and after the flushing experiments to examine changes in the element composition of the sediment. X-ray diffraction measurements were performed on the fine fractions of five sediment samples before the flushing experiment, following the methodology in Petschick et al. (1996), to assess clay mineralogy.

2.2. Flushing experiments

The main objective of the flushing experiments was to fully flush out the seawater from the sediment sample, replace it with freshwater, and assess changes in the sediment's geotechnical properties. The set-up for the flushing experiments is shown in Fig. 1. There are three pressure valves attached to a test chamber in a triaxial cell (cell pressure valve, back pressure valve, and pore water pressure valve). All these valves were open during the flushing process. The Automatic Pressure Controller (APC) was connected to the cell pressure and pore water pressure valves, while the back pressure valve was opened to allow water to flush and collect in the measuring cylinder. To flush the seawater out of the sample, both pressures from the cell and back were applied to the sediment, with values of 15 kPa and 10 kPa respectively. A low effective stress of 5 kPa was thus applied to ensure water flow while maintaining the original physical state of the sediment specimen.

Distilled water and three sediment samples were used during the flushing experiments. The sediment sample had a diameter and height of 3.8 and 8.4 cm, respectively. The cumulative duration of all the flushing experiments was three months. Flushing was performed until the

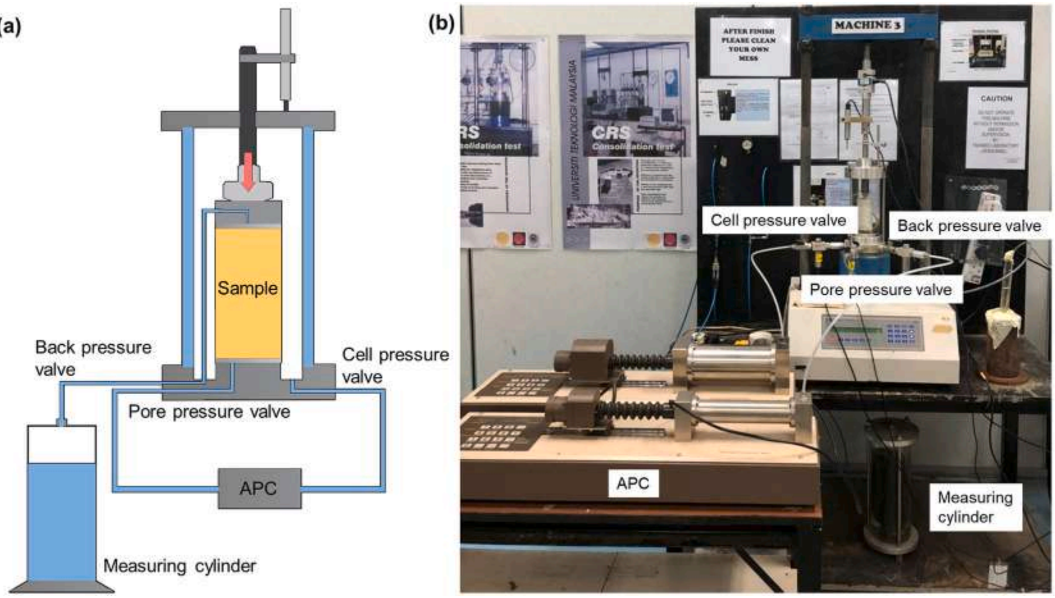

Fig. 1. (a) Schematic drawing of the experimental set-up used in this study (APC = Automatic Pressure Controller), b) Photograph of the experimental set-up in the laboratory.

salinity of the water seeping from the sample was <0.5 ppt and the pH value had decreased to 7.7. This was determined using a YSI model 30 salinity, conductivity and temperature sensor, and a pH meter. At the end of the experiments, the UU test was carried out on three saturated samples subjected to different confining pressures in the range of 100–600 kPa, following the ASTM D4767 standard. These pressures are slightly lower than those used for the samples before the flushing experiments because the flushing process decreased the plastic index and made the sample softer.

2.3. 2D numerical modelling

2D numerical modelling was carried out to assess the impact of changes in geotechnical properties associated with salt leaching on seafloor stability. Estimation of the factor of safety (FS) was performed using Slide2, a commercial slope stability software by Rocscience (*Rocscience*, 2020).

2.3.1. Governing equations

The finite element code is based on the limit equilibrium method for static and pseudo-static drained conditions that assumes an "infinite" slope. The equation that was used to calculate the FS is derived from Dugan and Flemings (2002):

$$FS = \frac{c_u' + \gamma' z(cos^2\theta - \lambda^*)tan\phi'}{\gamma' z sin\theta cos\theta} \quad (1)$$

where θ (^{0}) is the slope angle (also the angle of the slip surface), λ^* is the overpressure ratio ($\lambda^* = \Delta u/\delta'_{vh}$), u is the pore water pressure ($u = \rho_w gz$), δ'_{vh} is the hydrostatic vertical effective stress ($\delta'_{vh} = \rho_s gz$), c_u' (Pa) is the effective undrained cohesive strength, ϕ' (^{0}) is the effective soil friction angle, γ' (kN/m^3) is the effective soil unit weight ($\gamma' = \rho_s g$), ρ_s is sediment density, ρ_w is fluid density, z (m) is sub-seafloor depth and g is gravitational acceleration. The numerator of this equation originates from the Mohr-Coulomb failure criterion, where τ (Pa) is shear strength and σ'_n (Pa) is effective normal stress (Hampton et al., 1996). FS > 1 is indicative of slope stability whereas FS < 1 denotes slope instability.

The Slide2 model simulations were based on a non-circular surfaces-block search to estimate FS along linear and non-linear weak layers. For this purpose, we simulated the flushed state of clayey silt as a weak layer surrounded by the original state of the clayey silt sediments.

2.3.2. Simulations

The FS was estimated using the geotechnical properties (strength parameters, density, permeability) of the cored sediment sample before and after flushing. We considered a domain with dimensions of 300 m by 100 m and an overall slope gradient of 4°, which was represented by a finite element mesh with 10,000 triangular elements (each triangle having sides 2.5 m long). The entire slope is made of clayey silt saturated by seawater and located at a bathymetric depth of 100 m at its shallowest. Three different scenarios were considered where a 5 m thick layer of sediment was flushed with groundwater: (i) flushed layer is located at the surface, (ii) flushed layer is located at 25 m below seafloor, and (iii) flushed layer is located at 50 m below seafloor.

A sensitivity analysis was carried out to determine the effect of different slope gradients and thickness of the flushed layer on slope stability after flushing. Slope gradients were varied between 2.5 and 4°, whereas the thickness of the flushed layer was varied between 1 and 10 m.

3. Results

3.1. Sample characteristics

The Atterberg limits and particle size distribution of the sediment samples are presented in Table 2 and Fig. 2a. Based on these characteristics, the seafloor sediment can be classified as clayey silt with

Table 2
Atterberg limits and particle size distribution of the sediment samples.

Atterberg limits			
Sample	Liquid Limit (%)	Plastic Limit (%)	Plastic Index
Sample 1	33.25	17.06	16.18
Sample 2	38.21	18.32	19.89
Mean	35.73	17.69	18.04

Particle size distribution (by mass)		
Sand (0.075–4.75 mm) (%)	Silt (0.002–0.075 mm) (%)	Clay (< 0.002 mm) (%)
19.66	41.53	32.35

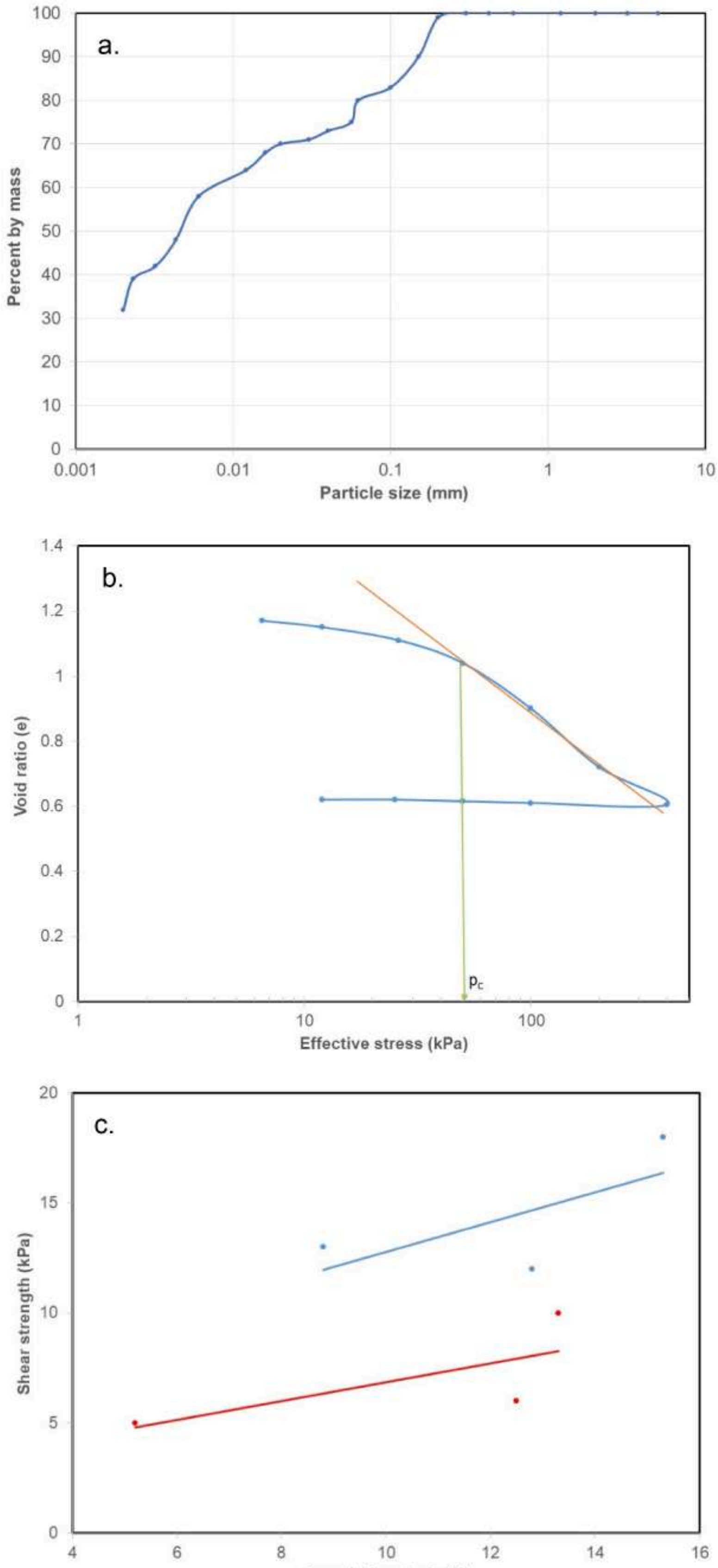

Fig. 2. (a) Particle size distribution of the sediment sample. (b) *E*-log *p* curve from the consolidation test. The blue line is the experimental data of void ratio and consolidation pressure. The orange line is the graphical procedure to find the gradient of the line that yields the compression index. p_c is the preconsolidation value of effective stress. (c) Plot of the cumulative strain vs. shear strength, before (in blue) and after (in red) the flushing experiments, derived from the triaxial test. (For interpretation of the references to colour in this figure legend, the reader is referred to the web version of this article.)

intermediate plasticity. The moisture content obtained from the samples ranges between 41.96% and 52.91%, with the optimal moisture content at 33.5%. The mean maximum dry density was 1.91 g/cm^3. Fig. 2b shows a plot of the void ratio vs. pressure for the loading and unloading phases. The preconsolidation stress (p_c) experienced by the sediment sample during the consolidation test is 50 kPa The compression indices Cc and Cr, obtained from the slope of the linear portion of the e-log p curve, are 0.519 and 0.021, respectively. The quality of the sample was determined by estimating the ratio $\Delta e/e_0$ (Fig. 2b); the estimated value is 0.07, which is equivalent to a "good to fair" sample quality category (Lunne et al., 2006). The permeability tests yielded a mean value of 1×10^{-14} m^2. The in situ total stress and hydrostatic pressure where the sample was collected are estimated at 262 kPa and 245 kPa, respectively. We did not measure in situ temperature, but this tends to be in the range of 4–5 °C (Kankaanpää et al., 2022).

3.2. Experimental results

3.2.1. Water chemistry

The changes in pH and salinity during the flushing experiments are presented in Fig. 3. We observe that the rate of salinity and pH of leachates in all tests decreases linearly. For all samples, three flushing cycles (with one cycle equivalent to 95.28 ml of water), were required to reach a salinity of 0.5 ppt and a pH of 7.7.

3.2.2. Geotechnical properties

The results from the UU tests before and after the flushing experiments are shown in Table 3. The UU tests before the flushing experiments were conducted with confining pressures of 200 kPa, 300 kPa, and 600 kPa, whereas those after the flushing experiments were conducted with confining pressures of 100 kPa, 200 kPa, and 600 kPa. After the flushing experiments we observe a decrease in the mean undrained cohesive strength, shear strength, bulk density and moisture content (Table 3). The ratio of undrained shear strength before leaching to that after leaching is equal to 2, which indicates that the sample was medium sensitive. No change in the volume of the sediment sample was measured during the flushing experiments.

A plot of the cumulative strain vs. shear strength, before and after the flushing experiments, is shown in Fig. 2c. Salt removal by the flushing process has resulted in a reduction in the elastic deformation parameters, which implies the development of a deformation band at the lower yield point.

3.2.3. Mineralogy

Fig. 4 shows the mean EDX measurements for sediment samples before and after the flushing experiments. The main elements in our samples are O, Si and C. After the flushing experiment, we note an increase in the concentration of O (6.1%), Si (2.1%), C (0.7%), and Ti (0.1%), and a decrease in the concentration of Al (2.3%), Fe (2.6%), K (1.1%), Mg (0.3%), Ca (2.9%), Cl (0.4%) and Na (1.0%). The X-ray diffraction measurements show that the clay fraction of our sediment samples consists of 65% illite, 15% chlorite and 15 kaolinite. Smectite was almost absent (<5%).

3.3. Slope stability models

3.3.1. Slope stability simulations

The slopes in all scenarios considered are initially stable, with a FS of >2. Following flushing of a 5 m thick sedimentary layer, the estimated FS for the three scenarios decreases to <1, denoting unstable conditions along the flushed layer (Fig. 5). The flushed sedimentary layer acts as a weak layer.

3.3.2. Sensitivity analysis

(a) Thickness of flushed layer

By plotting the thickness of the flushed layer against the estimated FS for the three different depths considered (0 m, 25 m, 50 m), we observe that an increase in the thickness of the flushed layer results in a decrease in FS (Fig. 6). The minimum thickness of the flushed layer for slope instability appears to range between 3.5 m (at 50 m depth) and 5 m (at the surface).

(b) Slope gradient

As shown in Fig. 7, slope failure occurred when the gradient was at least 3.8°, 3.0° and 3.0° for a flushed layer located at the surface, 25 m below seafloor and 50 m below seafloor, respectively.

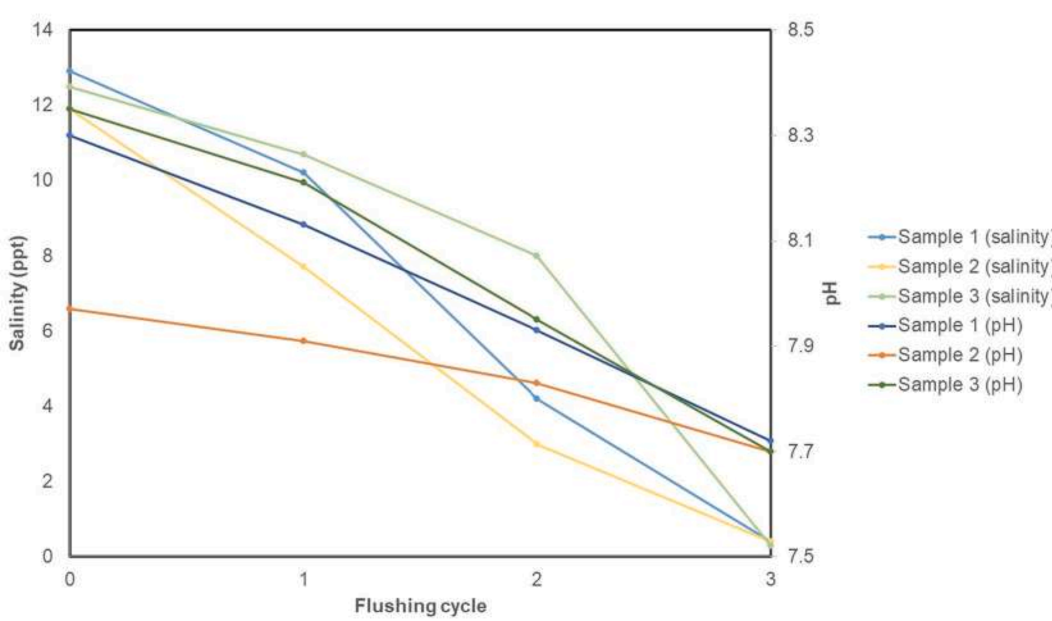

Fig. 3. Changes in the salinity (ppt) and pH during the experiments. Flushing cycle "0" denotes the starting conditions.

Table 3
Material parameters measured before and after the flushing experiment.

State	Sample	Cell pressure (kPa)	Maximum corrected deviator stress (kPa)	Undrained cohesive strength (c_u, kPa)	Mean undrained cohesive strength (c_u, kPa)	Mean shear strength (kPa)	Mean bulk density (g/cm^3)	Moisture content (%)
Before flushing	Sample 1	200	26	13	14.3	18	1.75	52.91
	Sample 2	300	25	12				
	Sample 3	600	37	18				
After flushing	Sample 1	100	10	5	7	10	1.50	41.96
	Sample 2	200	13	6				
	Sample 3	600	20	10				

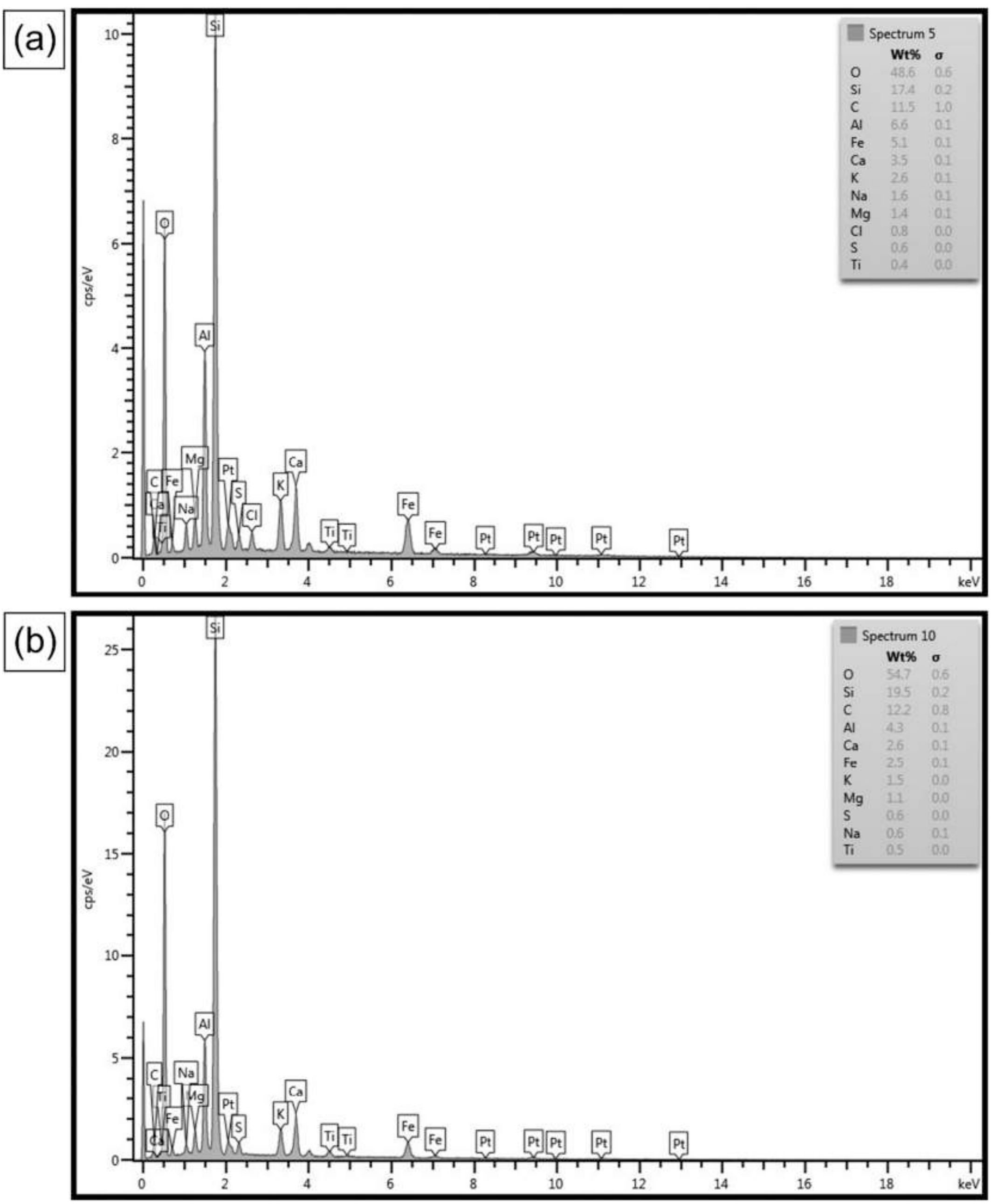

Fig. 4. EDX measurements of a sediment sample (a) before and (b) after the flushing experiment.

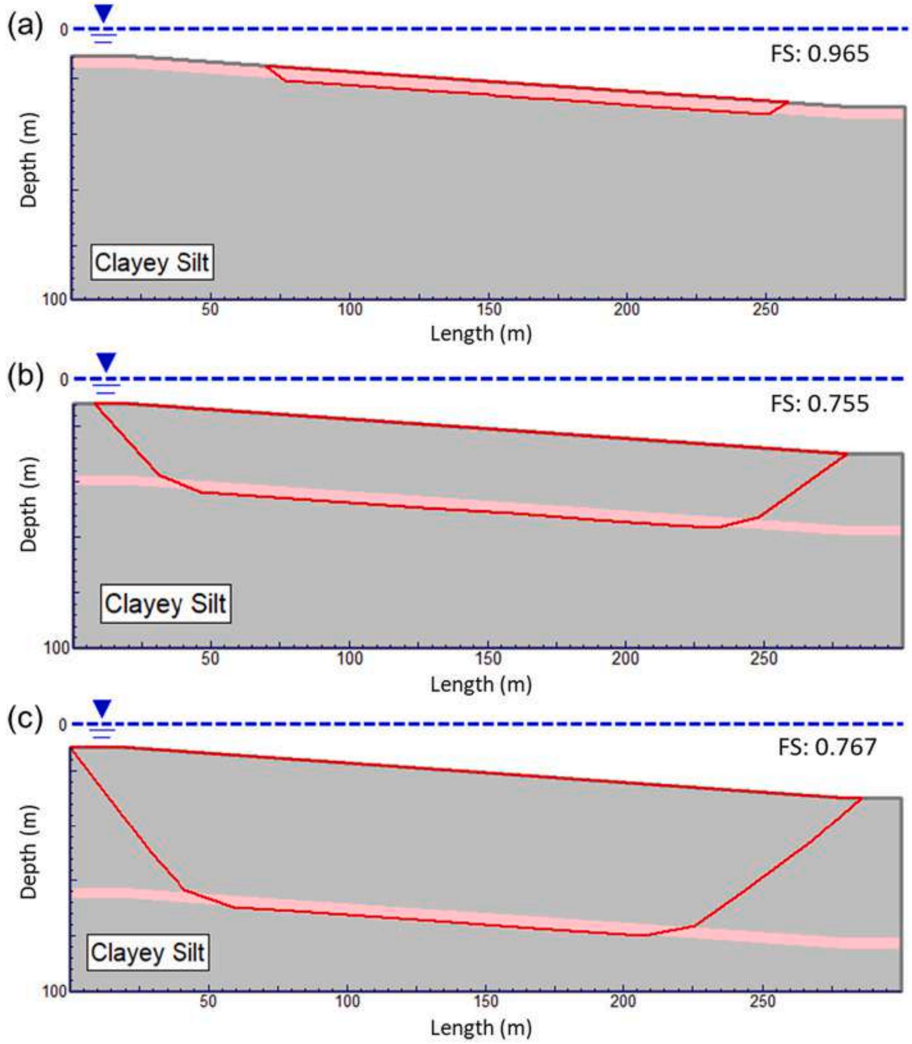

Fig. 5. Estimated factor of safety (FS) for three different scenarios where a 5 m thick layer of sediment was flushed with groundwater (denoted in pink): (a) flushed layer is located at the surface, (b) flushed layer is located at 25 m below seafloor, and (c) flushed layer is located at 50 m below seafloor. The dashed blue line is the water surface whereas the red line shows the failure surface. (For interpretation of the references to colour in this figure legend, the reader is referred to the web version of this article.)

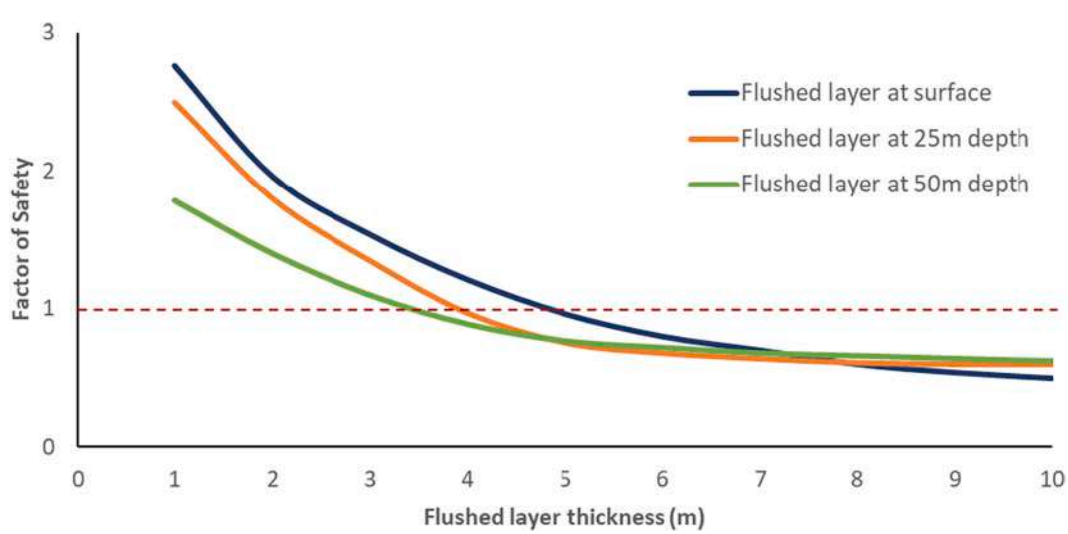

Fig. 6. Estimated factor of safety (FS) for different thicknesses of the flushed layer at a range of depths, for a slope gradient of 4°.

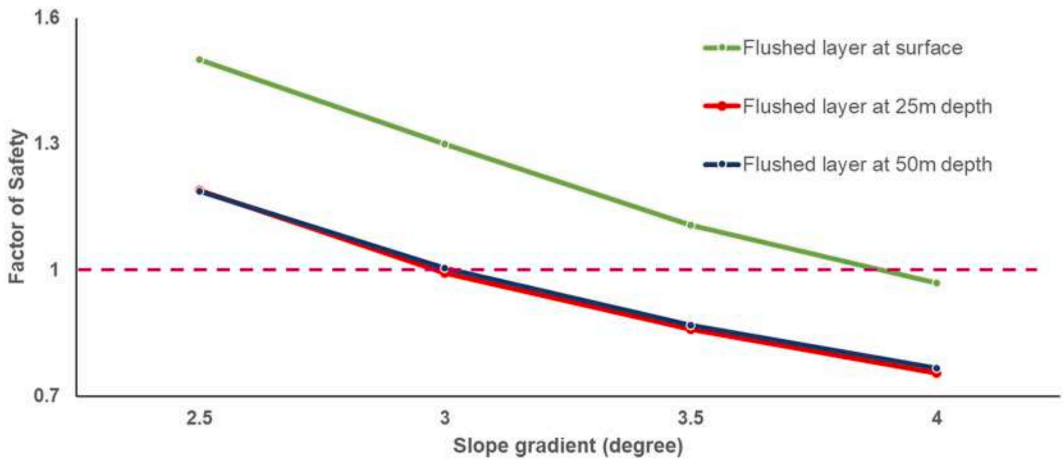

Fig. 7. Estimated factor of safety (FS) for different slope gradients for different depths of a flushed layer 5 m in thickness.

4. Discussion

4.1. Comparison with results from experiments on subaerial quick clays

The replacement of seawater by freshwater in the pores of our seafloor clayey silt samples results in a decrease in their undrained cohesive strength, shear strength, bulk density, and moisture content. Comparable changes in the same geotechnical parameters have been observed in subaerial quick clays that underwent salt leaching (Table 4). These studies have also reported how liquid limit, preconsolidation stress, and void ratio decreased after leaching, whereas the compression index, swelling index, and settlement increased after leaching (Table 4). We were unable to measure changes in these parameters because the sediment sample was too soft to handle at the end of the experiments. A decrease in Cl and Na concentrations in the sediment after leaching, as observed in Fig. 4, was also reported in marine clays by Liu et al. (2021).

4.2. Implications for slope failure by OFG flow/seepage in continental margins

The results from our laboratory experiments and numerical models demonstrate that, by reducing the cohesive and shear strength of clayey silts, salt leaching can trigger failure in siliciclastic continental margins. In the considered scenarios, failure can be triggered by salt leaching where the thickness of the flushed layer is >3.5 m or where the slope gradient is >3°. The settings that are conducive to failure by salt leaching are therefore the relatively steep parts of continental margins that are rich in clay-silt sediments and that undergo groundwater flushing. These primarily comprise: (i) the continental slope, either during sea-level lowstands and/or where the shelf is narrow, or (ii) the shallow seafloor between the shoreline and the upper shelf, which experiences the longest salt leaching episodes during a single glacial cycle and where the most active recharge by freshwater occurs at present. The 1979 Nice harbour landslide site, where salt leaching had been proposed as a potential mechanism for sediment weakening, creep, and microslumping (e.g. Dan et al., 2007; Kopf et al., 2016; Stegmann et al., 2011), fits the latter criteria. The site is located close to the coast at water depths of <50 m. Freshwater infiltration by precipitation, river discharge and snow melt recharge sandy and clay layers at the scar wall, increasing clay sensitivity and decreasing the effective stress. In other parts of the continental margin, where slope gradients are <3° (e.g. middle to our shelf) or where the flushed layer is <3.5 m thick, OFG flow/seepage is expected to only precondition the slope to failure.

There are a number of sites globally where OFG has been associated to seafloor geomorphic change. These primarily include continental shelf to slope environments in siliciclastic margins, where OFG flow and seepage have been proposed to drive slope failure (Beaufort Sea, Canada (Paull et al., 2021)), canyon erosion (KwaZuluNatal, South Africa (Green and Uken, 2008); Alías-Almanzora canyon system, Spain (Puig et al., 2017)) and pockmark formation (Beaufort Sea, Canada (Gwiazda et al., 2018); New England Mud Patch, NE USA (Goff, 2019); Baltic Sea (Jakobsson et al., 2020)). The inferred influence of OFG in such settings is mechanical, either by lowering the effective stress of sediment via the generation of excess pore pressure (Sultan et al., 2020), or via the exertion of a seepage force that offsets the frictional forces within the sediments (Pratson et al., 2009). There is no reason to preclude salt leaching as an additional factor driving instability in the continental slope sites, or preconditioning the slope to failure in the continental shelf

Table 4
Comparison of our results with those from experiments carried out on subaerial quick clays.

Parameters	Before leaching (our experiments)	After leaching (our experiments)	Before leaching (literature	After leaching (literature)	Reference
Compression index, Cc	0.519		0.15	0.21	(Nagase et al., 2006)
Liquid limit (%)	35.73		43.4	27.4	(Bjerrum, 1954)
Preconsolidation stress, σpc' (kPa)	50		50	45	(Ismael, 1993)
Undrained shear strength (kPa)	14.3	7.00	19.6	9.8	(Bjerrum, 1967)
Ratio of undrained shear strength to effective overburden pressure	0.14	0.07	0.16–0.25	0.09–0.12	(Bjerrum, 1967)
Remoulded shear strength (kPa)			0.25–0.9	0.5	(He et al., 2015)
Settlement (vertical strain, %)			1.5	4.5	(Kazi and Moum, 1972)
Swelling index, Cs			0.001	0.015	(Nagase et al., 2006)
Unit weight, γ (g/cm^3)	1.75	1.50	1.69	1.57	(Ismael, 1993)
Void ratio, e_0	1.04		0.45	0.42	(Azam, 2000)

sites (primarily in relation to pockmark formation).

Another important factor controlling the impact of salt leaching by OFG on slope stability is the extent of groundwater flushing. This tends to be higher in settings with wet climates, steep coastal topographies (more common in active margins), and permeable sediments in the upper shelf (which would facilitate flushing and salinisation). There are 305 records of OFG in continental margins globally (Micallef et al., 2021). Of these:

i. 76% were emplaced by meteoric or glacial recharge;
ii. 31% are located in continental slopes; with the remaining 69% in continental shelves;
iii. ~26% are located at a sub-seafloor depth of 0–50 m and have a thickness of 0–250 m;
iv. Where the aquifer type is known, 31% occur in clays and/or silts.

This means that, based on the inferences made in our study, one-third of known OFG sites should be conducive to slope instability due to salt leaching related to OFG flow. It is worth mentioning that since the preservation potential of OFG can be in the range 30–45% of the initial OFG volume (as estimated for the New Jersey margin after 12 ka (Thomas et al., 2019)), salt leaching, and possibly slope failure, in the continental slope are expected to have reoccurred during every glacial cycle.

4.3. Limitations and sources of error

The main limitations of our study include: (i) The range of pore water salinity used is limited in comparison to what can be encountered in the field. (ii) In the field, groundwater pressures may be higher than those applied in the laboratory. (iii) We did not consider the impact of sediment compaction on changes in the shear strength with depth in the numerical model. The likelihood of slope failure occurring where the flushed layer is located at depth is thus lower than estimated by our model. (iv) We did not assess the impact of mesh size on the modelling results, although we did use a fine enough mesh to resolve the flushed layer with at least two elements. (v) The geology of the continental margin considered in the numerical model is simplified, as we did not consider heterogeneities associated to sediment variability or erosional/depositional structures, both of which are typical of siliciclastic continental margins.

The main sources of error during the flushing experiments were: (i) The error in the sensor reading (vertical measurement, pressure transducer). These were in the range of ± 5 kPa, but were minimised by having the readings automatically logged by a data logger. (ii) The magnitude of pore pressure change during the experiment, which could not be measured.

5. Conclusions

Flushing experiments have shown that replacement of seawater by freshwater in the pores of seafloor clayey silt can decrease the undrained cohesive strength by 50%, as well as a decrease in its shear strength, bulk density, and moisture content. This is comparable to observations made in salt leaching experiments using subaerial quick clays. 2D limit equilibrium modelling of a theoretical submarine slope domain 300 m by 100 m demonstrates that salt leaching by OFG flow can trigger slope failure where the thickness of the flushed layer is >3.5 m or when the slope gradient is >3°. The settings that are most likely to be impacted by slope failure due to salt leaching are the shallow seafloor close to the shoreline, and the continental slope. Elsewhere along the continental margin, OFG flow/seepage is expected to precondition the slope to failure. One-third of known OFG sites is likely conducive to slope instability due to salt leaching related to OFG flow. Salt leaching associated with OFG flow/seepage merits to be considered with overpressure generation as a potential mechanism destablising submarine sedimentary slopes and driving seafloor geomorphic change.

Declaration of Competing Interest

The authors declare the following financial interests/personal relationships which may be considered as potential competing interests:

Aaron Micallef reports financial support was provided by European Research Council.

Data availability

The data supporting the findings of this study are available via this link: https://figshare.com/s/cc020f8742412e93668e.

Acknowledgments

This project has received funding from the European Research Council (ERC) under the European Union's Horizon 2020 research and innovation programme (grant agreement No 677898 (MARCAN)). We thank Jens Karstens and Christian Berndt for providing access to the sediment samples, as well as Frank Wuttke and Charlotte von Bismarck for assistance with sample preparation. We are grateful to Matt O'Regan and three anonymous reviewers for their insightful comments.

References

Azam, S., 2000. Collapse and compressibility behaviour of arid calcareous soil formations. Bull. Eng. Geol. Environ. 59, 211–217.
Barbour, S.L., Yang, N., 1993. A review of the influence of clay–brine interactions on the geotechnical properties of Ca-montmorillonitic clayey soils from western Canada. Can. Geotech. J. 30, 920–934.
Bintanja, R., Van de Wal, R.S.W., Oerlemans, J., 2005. Modelled atmospheric temperatures and global sea levels over the past million years. Nature 437, 125–128.
Bjerrum, L., 1954. Geotechnical properties of Norwegian marine clays. Géotechnique 4, 49–69.
Bjerrum, L., 1967. Engineering geology of Norwegian normally-consolidated marine clays as related to settlements of buildings. Géotechnique 17, 83–118.
Bull, S., Cartwright, J., Huuse, M., 2009. A subsurface evacuationmodel for submarine slope failure. Basin Res. 21, 433–443.
Cohen, D., Person, M., Wang, P., Gable, C.W., Hutchinson, D., Marksamer, A., Dugan, B., Kooi, H., Groen, K., Lizzarlde, D., Evans, R.L., Day-Lewis, F.D., Lane Jr., J.W., 2010. Origin and extent of freshwater paleowaters on the Atlantic continental shelf, USA. Groundwater 48, 143–158.
Dan, G., Sultan, N., Savoye, B., 2007. The 1979 Nice harbour catastrophe revisited: Trigger mechanism inferred from geotechnical measurements and numerical modelling. Mar. Geol. 245, 40–64.
Deng, Y.F., Cui, Y.J., Tang, A.M., Nguyen, X.P., Li, X.L., Van Geet, M., 2011. Investigating the pore-water chemistry effects on the volume change behaviour of Boom clay. Phys. Chem. Earth, Parts A/B/C 36, 1905–1912.
Dugan, B., Flemings, P.B., 2002. Fluid flow and stability of the US continental slope offshore New Jersey from the Pleistocene to the present. Geofluids 2, 137–146.
Dutkiewicz, A., Müller, R.D., O'Callaghan, S., Jónasson, H., 2015. Census of seafloor sediments in the world's ocean. Geology 43, 795–798.
Faure, H., Walter, R.C., Grant, D.R., 2002. The coastal oasis: ice age springs on emerged continental shelves. Glob. Planet. Chang. 33, 47–56.
Goff, J.A., 2019. Modern and fossil pockmarks in the New England Mud Patch: Implications for submarine groundwater discharge on the middle shelf. Geophys. Res. Lett. 46, 12213–12220.
Green, A., Uken, R., 2008. Submarine landsliding and canyon evolution on the northern KwaZuluNatal continental shelf, South Africa. Mar. Geol. 254, 152–170.
Gwiazda, R., Paull, C.K., Dallimore, S.R., Melling, H., Jin, Y.K., Hong, J.K., Riedel, M., Lundsten, E., Anderson, K., Conway, K., 2018. Freshwater seepage into sediments of the shelf, shelf edge, and continental slope of the Canadian Beaufort Sea. Geochem. Geophys. Geosyst. 19.
Hampton, M.A., Lee, H.J., Locat, J., 1996. Submarine landslides. Rev. Geophys. 34, 33–59.
Haroon, A., Micallef, A., Jegen, M., Schwalenberg, K., Karstens, J., Berndt, C., Garcia, X., Kuehn, M., Rizzo, E., Fusi, N.C., Ahaneku, C.V., Petronio, L., Faghih, Z., Weymer, B. A., De Biase, M., Chidichimo, F., 2021. Electrical resistivity anomalies offshore a carbonate coastline: evidence for freshened groundwater? Geophys. Res. Lett. 48 (14) e2020GL091909.
Hay, W.W., Leslie, M., 1985. Pore space in sediments on continental blocks and sea level change. Geol. Soc. Am. Abstr. Programs 17, 605.
He, P., Ohtsubo, M., Higashi, T., Kanayama, M., 2015. Sensitivity of salt-leached clay sediments in the Ariake Bay Area, Japan. Mar. Georesour. Geotechnol. 33, 429–436.
Hillman, J.I.T., Gorman, A.R., Pecher, I., 2015. Geostatistical analysis of seafloor depressions on the southeast margin of New Zealand's South Island — investigating

the impact of dynamic near seafloor processes on geomorphology. Mar. Geol. 360, 70–83.

Hoffmann, J.J.L., Schneider von Deimling, J., Schröder, J.F., Schmidt, M., Held, P., Crutchley, G.J., Scholten, J., Gorman, A.R., 2020. Complex eyed pockmarks and submarine groundwater discharge revealed by acoustic data and sediment cores in Eckernförde Bay, SW Baltic Sea. Geochem. Geophys. Geosyst. 21, 1–18.

Hübscher, C., Borowski, C., 2006. Seismic evidence for fluid escape from Mesozoic cuesta type topography in the Skagerrak. Mar. Pet. Geol. 23, 17–28.

Idczak, J., Brodecka-Goluch, A., Łukawska-Matuszewska, K., Graca, B., Gorska, N., Klusek, Z., Pezacki, P.D., Bolałek, J., 2020. A geophysical, geochemical and microbiological study of a newly discovered pockmark with active gas seepage and submarine groundwater discharge (MET1-BH, central Gulf of Gdańsk, southern Baltic Sea). Sci. Total Environ. 742, 140306.

Ismael, N.F., 1993. Laboratory and field leaching tests on coastal salt-bearing soils. J. Geotech. Eng. 119, 453–470.

Jakobsson, M., O'Regan, M., Mörth, C.M., Stranne, C., Weidner, E., Hansson, J., Gyllencreutz, R., Humborg, C., Elfwing, T., Norkko, A., 2020. Potential links between Baltic Sea submarine terraces and groundwater seeping. Earth Surf. Dyn. 8, 1–15.

Jensen, J.B., Kuijpers, A., Bennike, O., Laier, T., Werner, F., 2002. New geological aspects for freshwater seepage and formation in Eckernförde Bay, western Baltic. Cont. Shelf Res. 22, 2159–2173.

Johnson, D.W., 1939. The Origin of Submarine Canyons: A Critical Review of Hypotheses. Columbia University Press, New York.

Kankaanpää, H.T., Alenius, P., Kotilainen, P., Roiha, P., 2022. Decreased surface and bottom salinity and elevated bottom temperature in the Northern Baltic Sea over the past six decades. Sci. Total Environ. 160241.

Kazi, A., Moum, J., 1972. Effect of Leaching on the Fabric of Normally Consolidated Marine Clays. International Symposium on Soil Structure, Gothenburg, pp. 137–152.

Kelner, M., Migeon, S., Tric, E., Couboulex, F., Dano, A., Lebourg, T., Taboada, A., 2014. Recent morphological changes of the Nice continental slope. In: Lollino, G. (Ed.), Engineering Geology for Society and Territory. Springer International Publishing, Switzerland, pp. 221–225.

Kim, Y.-T., Do, T.-H., 2011. Experimental Evaluation of Leaching Effects on the Compressibility of Marine Clay and its Strain Rate Dependency. Mar. Georesour. Geotechnol. 29, 16–29.

Kohout, F.A., Cooper, H.H.F.A.K., Henry, H.H., Glover, R.E., 1964. The flow of fresh water and salt water in the Biscayne aquifer of the Miami area, Florida. In: Sea Water in Coastal Aquifers: Relation of Salt Water to Fresh Groundwater. USGS Watersupply. C12-33.

Kooi, H., Groen, K., 2001. Offshore continuation of coastal groundwater systems; predictions using sharp-interface approximations and variable-density flow modelling. J. Hydrol. 246, 19–35.

Kooi, H., Groen, J., Leijnse, A., 2000. Modes of seawater intrusion during transgressions. Water Resour. Res. 36, 3581–3589.

Kopf, A., Stegmann, S., Garziglia, S., Henry, P., Dennielou, B., Haas, S., Weber, K.C., 2016. Soft sediment deformation in the shallow submarine slope off Nice (France) as a result of a variably charged Pliocene aquifer and mass wasting processes. Sediment. Geol. 344, 290–309.

La Rochelle, P., Chagnon, J.Y., Lefebvre, G., 1970. Regional geology and landslides in the marine clay deposits of eastern Canada. Can. Geotech. J. 7, 145–156.

Leahy, P.P., Meisler, H., 1982. An analysis of fresh and saline ground water in the New Jersey Coastal Plain and continental shelf. EOS Trans. Am. Geophys. Union 63, 322.

L'Heureux, J.S., Hansen, L., Longva, O., Emdal, A., Grande, L., 2010. A multidisciplinary study of submarine landslides at the Nidelva fjord delta, Central Norway - Implications for geohazard assessment. Nor. Geogr. Tidsskr. 90, 1–20.

L'Heureux, J.-S., Longva, O., Steiner, A., Hansen, L., Vardy, M.E., Vanneste, M., Haflidason, H., Brendryen, J., Kvalstad, T.J., Forsberg, C.F., Chand, S., Kopf, A., 2012. Identification of weak layers and their role for the stability of slopes at Finneidfjord, Northern Norway. In: Yamada, Y., Kawamura, K., Ikehara, K., Ogawa, Y., Urgeles, R., Mosher, D., Chaytor, J., Strasser, M. (Eds.), Submarine Mass Movements and their Consequences. Springer, Netherlands, Dordrecht, pp. 321–330.

Liu, J., Afroz, M., Ahmad, A., 2021. Experimental investigation of the impact of salinity on Champlain Sea clay. Mar. Georesour. Geotechnol. 39, 494–504.

Locat, J., Demers, D., 1988. Viscosity, yield stress, remolded strength, and liquidity index relationships for sensitive clays. Can. Geotech. J. 25, 799–806.

Lunne, T., Berre, T., Andersen, K.H., Strandvik, S., Sjursen, M., 2006. Effects of sample disturbance and consolidation procedures on measured shear strength of soft marine Norwegian clays. Can. Geotech. J. 43, 726–750.

Madadzadeh Toulegilan, M., Jamshidi Chenari, R., Lashteh Neshaei, M.A., Forghani, A., 2020. Changes in stability conditions of clay slopes due to leaching: a case study. SN Appl. Sci. 2, 1031.

Micallef, A., Person, M., Haroon, A., Weymer, B.A., Jegen, M., Schwalenberg, K., Faghih, Z., Duan, S., Cohen, D., Mountjoy, J.J., Woelz, S., Gable, C.W., Averes, T., Tiwari, A.K., 2020. 3D characterisation and quantification of an offshore freshened groundwater system in the Canterbury Bight. Nat. Commun. 11, 1372.

Micallef, A., Person, M., Berndt, C., Bertoni, C., Cohen, D., Dugan, B., Evans, R., Haroon, A., Hensen, C., Jegen, M., Key, K., Kooi, H., Liebetrau, V., Lofi, J., Mailloux, B.J., Martin-Nagle, R., Michael, H.A., Muller, T., Schmidt, M., Schwalenberg, K., Trembath-Reichert, E., Weymer, B., Zhang, Y., Thomas, A.T., 2021. Offshore freshened groundwater in continental margins. Rev. Geophys. 59 e2020RG000706.

Moernaut, J., Wiemer, G., Reusch, A., Stark, N., De Batist, M., Urrutia, R., Ladron de Guevara, B., Kopf, A., Strasser, M., 2017. The influence of overpressure and focused fluid flow on subaquatic slope stability in a formerly glaciated basin: Lake Villarrica (South-Central Chile). Mar. Geol. 383, 35–54.

Morrissey, S.K., Clark, J., Bennett, M., Richardson, E., Stute, M., 2010. Groundwater reorganization in the Floridan aquifer following Holocene Sea-level rise. Nat. Geosci. 3, 683–687.

Müller, H., von Dobeneck, T., Nehmiz, W., Hamer, K., 2011. Near-surface electromagnetic, rock magnetic, and geochemical fingerprinting of submarine fresh water seepage at Eckernförde Bay (SW Baltic Sea). Geo-Mar. Lett. 31, 123–140.

Nagase, H., Shimizu, K., Hiro-oka, A., Tanoue, Y., Saitoh, Y., 2006. Earthquake-induced residual deformation of Ariake clay deposits with leaching. Soil Dyn. Earthq. Eng. 26, 209–220.

Nardin, T.R., Hein, F.J., Gorsline, D.S., Edwards, B.D., 1979. A review of mass movement processes, sediment and acoustic characteristics, and contrasts in slope and base-of-slope systems versus canyon-fan-basin floor systems. Soc. Econ. Paleontol. Mineralog. Spe. Pub. 27, 61–73.

Nguyen, X.P., Cui, Y.J., Tang, A.M., Deng, Y.F., Li, X.L., Wouters, L., 2013. Effects of pore water chemical composition on the hydro-mechanical behavior of natural stiff clays. Eng. Geol. 166, 52–64.

Oehler, T., Mogollon, J.M., Moosdorf, N., Winkler, A., Kopf, A., Pichler, T., 2017. Submarine groundwater discharge within a landslide scar at the French Mediterranean coast. Estuar. Coast. Shelf Sci. 198, 128–137.

Paull, C.K., Dallimore, S.R., Caress, D.W., Gwiazda, R., Lundsten, E., Anderson, K., Melling, H., Jin, Y.K., Duchesne, M.J., Kang, S.G., Kim, S., Riedel, M., King, E.L., Lorenson, T., 2021. A 100-km wide slump along the upper slope of the Canadian Arctic was likely preconditioned for failure by brackish pore water flushing. Mar. Geol. 435, 106453.

Person, M., Dugan, B., Swenson, J., Urbano, L., Stott, C., Taylor, J., Willett, M., 2003. Pleistocene hydrogeology of the Atlantic continental shelf, New England. Geol. Soc. Am. Bull. 115, 1324–1343.

Petschick, R., Kuhn, G., Gingele, F., 1996. Clay mineral distribution in surface sediments of the South Atlantic: sources, transport, and relation to oceanography. Mar. Geol. 130, 203–229.

Post, V.E.A., Groen, J., Kooi, H., Person, M., Ge, S., Edmunds, W.M., 2013. Offshore fresh groundwater reserves as a global phenomenon. Nature 504, 71–78.

Pratson, L.F., Nittrouer, C.A., Wiberg, P.L., Steckler, M.S., Swenson, J.B., Cacchione, D. A., Karson, J.A., Murray, A.B., Wolinsky, M.A., Gerber, T.P., Mullenbach, B.L., Spinelli, G.A., Fulthorpe, C.S., O'Grady, D.B., Parker, G., Driscoll, N.W., Burger, R.L., Paola, C., Orange, D.L., Field, M.E., Friedrichs, C.T., Fedele, J.J., 2009. Seascape evolution on clastic continental shelves and slopes. In: Nittrouer, C.A., Austin, J.A., Field, M.E., Kravitz, J.H., Syvitski, J.P.M., Wiberg, P.L. (Eds.), Continental Margin Sedimentation: From Sediment Transport to Sequence Stratigraphy: IAP Special Publication. Blackwell Publishing, Oxford, pp. 339–380.

Puig, P., Duran, R., Munoz, A., Elvira, E., Guillen, J., 2017. Submarine canyon-head morphologies and inferred sediment transport processes in the Alías-Almanzora canyon system (SW Mediterranean): on the role of the sediment supply. Mar. Geol. 393, 21–34.

Rise, L., Saettem, J., Fanavoll, S., Thorsnes, T., Ottensen, D., Boe, R., 1999. Sea-bed pockmarks related to fluid migration from Mesozoic bedrock strata in the Skagerrak offshore Norway. Mar. Pet. Geol. 16, 619–631.

Rocscience, 2020.

Rolfe, P.F., Aylmore, L.A.G., 1977. Water and salt flow through compacted clays: I. Permeability of compacted illite and montmorillonite. Soil Sci. Soc. Am. J. 41, 489–495.

Stegmann, S., Sultan, N., Kopf, A., Apprioual, R., Pelleau, P., 2011. Hydrogeology and its effect on slope stability along the coastal aquifer of Nice, France. Mar. Geol. 280, 168–181.

Stetson, H.C., Smith, J.F., 1938. Behavior of suspension currents and mud slides on the continental slope. Am. J. Sci. 35, 1–13.

Sultan, N., Garziglia, S., Bompais, X., Woerther, P., Witt, C., Kopf, A., Migeon, S., 2020. Transient Groundwater flow through a coastal confined aquifer and its impact on nearshore submarine slope instability. J. Geophys. Res. Earth Surf. 125 e2020JF005654.

Thomas, A.T., Reiche, S., Riedel, M., Clauser, C., 2019. The fate of submarine fresh groundwater reservoirs at the New Jersey shelf, USA. Hydrogeol. J. 27 (7), 2673–2694.

Torrance, J.K., 1974. A laboratory investigation of the effect of leaching on the compressibility and shear strength of Norwegian marine clays. Géotechnique 24, 155–173.

Vanneste, M., Longva, O., L'Heureux, J.S., Vardy, M.E., Morgan, E., Forsberg, C.F., Kvalstad, T.J., Strout, J.M., Brendryen, J., Haflidason, H., Lecomte, I., Steiner, A., Kopf, A., Mörz, T., Kreiter, S., 2013. Finneidfjord, a field laboratory for integrated submarine slope stability assessments and characterization of landslide-prone sediments: a review. In: Offshore Technology Conference, Houston, Texas.

Virtasalo, J.J., Schröder, J.F., Luoma, S., Majaniemi, J., Mursu, J., Scholten, J., 2019. Submarine groundwater discharge site in the first Salpausselkä ice-marginal formation, South Finland. Hydrol. Earth Syst. Sci. 10, 405–423.

Whiticar, M.J., 2002. Diagenetic relationships of methanogenesis, nutrients, acoustic turbidity, pockmarks and freshwater seepages in Eckernförde Bay. Mar. Geol. 182, 29–53.

Wu, Z., Deng, Y., Chen, Y., Gao, Y., Zha, F., 2021. Long-term desalination leaching effect on compression/swelling behaviour of Lianyungang marine soft clays. Bull. Eng. Geol. Environ. 80, 8099–8107.

Zhang, T., Deng, Y., Cui, Y., Lan, H., Zhang, F., Zhang, H., 2019. Porewater salinity effect on flocculation and desiccation cracking behaviour of kaolin and bentonite considering working condition. Eng. Geol. 251, 11–23.